



AIAA 99-3788

**BOUNDARY-LAYER RECEPTIVITY TO
FREESTREAM DISTURBANCES AND
ITS ROLE IN TRANSITION (INVITED)**

W.S. Saric, E.B. White, and H.L. Reed

Arizona State University
MAE Dept. Box 876106
Tempe, AZ. 85287-6106
saric@asu.edu
<http://wtsun.eas.asu.edu>

30th AIAA Fluid Dynamics Conference
28 June - 1 July, 1999 / Norfolk, VA

For permission to copy or republish, contact the American Institute of Aeronautics and Astronautics
1801 Alexander Bell Drive, Suite 500, Reston, VA 20191

BOUNDARY-LAYER RECEPTIVITY TO FREESTREAM DISTURBANCES AND ITS ROLE IN TRANSITION

William S. Saric^{*}, Edward B. White⁺ and Helen L. Reed^{*}

Mechanical and Aerospace Engineering
Arizona State University
Tempe, Arizona 85287-6106

ABSTRACT

The current understanding of the receptivity of the leading edge to external disturbances is reviewed with special attention paid to the role of freestream sound. Only a brief review of the role of freestream turbulence and vorticity is given because progress has been slow in these areas. Recent advances in the theoretical modeling, direct numerical simulations, and experimental measurements are discussed. It is shown that aspects of the theory have been validated and the mechanisms of freestream disturbances providing the initial conditions for unstable waves is better understood.

NOMENCLATURE

a, b major and minor axes of an ellipse
 A norm of disturbance amplitude
 A_0 amplitude at $R = R_0$, usually Branch I
 AR aspect ratio of "elliptic" nose
 $F = \omega/Rx10^6 = 2\pi f/U_\infty^2 x10^6$: dimensionless frequency
 f dimensional frequency [Hz]
 $K_s = (|u'|_{TS})/(|u'|_{ac})_{f_s}$: receptivity coefficient referenced to branch I. Eq. (2)
 L length scale, chord [m]
 $M = U_\infty/c_a$: Mach number
 m, n exponents in super-ellipse equation. Eq. (1)

$N = \ln(A/A_0)$: amplification factor
 $R = (R_x)^{1/2} = U_\infty \delta_r / \nu$: boundary-layer Reynolds number
 R_0 initial boundary-layer Reynolds number, usually Branch I
 $R_L = U_\infty L / \nu$: chord Reynolds number
 $R_x = U_\infty x^* / \nu$: x -Reynolds number or chord Reynolds number
 r_n nose radius [m]
 $S = 2\pi f r_n / U_\infty$: Strouhal number based on nose radius
 U basic-state chordwise boundary-layer velocity normalized by U_∞
 U_∞ freestream velocity, [m/s]
 $|u'|$ rms of u' normalized by U_∞
 x, y, z chordwise, wall-normal, and spanwise coordinates normalized by δ_r
 x^*, y^*, z^* dimensional coordinates [m]
 $\alpha = \alpha_r + i\alpha_i$: chordwise complex wavenumber normalized by δ_r
 $\alpha_r = 2\pi\delta_r / \lambda_{TS}$
 $\alpha_{TS} = 2\pi\delta_r / \lambda_{TS}$
 α_{f_s} wavenumber of freestream disturbance
 α_{eff} effective angle of attack

^{*} Professor, Associate Fellow AIAA

⁺ NDFEG Fellow, Member AIAA

δ_r	$= (vx^*/U_\infty)^{1/2}$: boundary-layer reference length, [m], (normalizing length)
ε_{LE}	$= (2\pi f v / U_\infty^2)^{1/6} = 0.1F^{1/6}$: small acoustic parameter
η	$= y^* / \delta_r = y$: boundary-layer coordinate
θ	sound incidence angle
λ_{TS}	T-S wavelength [m]
μ	$= \alpha_{eff} (2L/r_n)^{1/2}$
ν	kinematic viscosity [m ² /s]
ρ	density [kg/m ³]
ω	$= 2\pi f \delta_r / U_\infty = FRx10^{-6}$: dimensionless circular frequency

1 INTRODUCTION

Understanding the origins of turbulent flow and transition from laminar to turbulent flow is still an important challenge of fluid mechanics. The common thread connecting aerodynamic applications is the fact that they deal with *bounded shear flows* (boundary layers) in *open systems* (with different upstream or initial amplitude conditions). It is well known that the stability, transition, and turbulent characteristics of bounded shear layers are fundamentally different from those of free shear layers (Morkovin 1969, 1978, 1983, 1991; Reshotko 1976; Bayley et al 1988). Likewise, the stability, transition, and turbulent characteristics of open systems are fundamentally different from those of closed systems. The distinctions are vital.

At the present time no mathematical model exists that can predict the transition Reynolds number on a flat plate. One obvious reason for this is the variety of influences such as freestream turbulence, surface roughness, sound, etc. which are incompletely understood, yet may trigger transition through a forced response of the flow as a nonlinear oscillator (Morkovin 1991). A second reason, of course, is the poor understanding of the free response of this nonlinear oscillator, i.e., of the fundamental mechanisms which lead initially small disturbances to transition. An important historical perspective of the progress, accomplishments, and issues in transition prediction is given by Reshotko (1997).

Important sources of information regarding aerodynamic applications of transition are found in various AGARD Special Courses. The most recent courses that are relevant to this problem are: *Stability and Transition of Laminar Flow* (AGARD Report No. 709, 1984); *Aircraft Drag Prediction and Reduction* (AGARD Report No. 723, 1985); *Skin Friction Drag Reduction* (AGARD Report No. 786, 1992); and *Progress in Transition Modelling* (AGARD Report No. 793, 1993).

Reed et al (1996) review the literature and discuss the importance of this work as it relates to aircraft skin-friction reduction, so much of this material is not repeated here. With the maturation of linear-stability methods and the conclusions that breakdown mechanisms are initial-condition dependent (Saric and Thomas 1984; Singer et al 1986, 1989; Corke 1990), more emphasis is now placed on the understanding of the source of initial disturbances than on the details of the latter stages of transition.

1.1 The Process of Transition for Boundary Layers in External Flows

In fluids, turbulent motion is usually observed rather than laminar motion because the Reynolds-number range of laminar motion is generally limited. The *transition* from laminar to turbulent flow occurs because of an incipient instability of the basic flow field. This instability intimately depends on subtle, and sometimes obscure, details of the flow. The process of transition for *boundary layers in external flows* can be qualitatively described using Fig.1 and the following (albeit, oversimplified) scenario based on one of the different “roadmaps” to turbulence developed over the years by Morkovin, Reshotko, and Herbert.

Disturbances in the freestream, such as sound or vorticity, enter the boundary layer as steady and/or unsteady fluctuations of the basic state. This part of the process is called *receptivity* (Morkovin, 1969) and although it is still not well understood, it provides the vital initial conditions of amplitude, frequency, and phase for the breakdown of laminar flow. In Fig. 1, the initial amplitude increases schematically from left to right. Initially these disturbances may be too small to measure and they are observed only after the onset of an instability. A number of different instabilities can occur independently or together and the appearance of any particular type of instability depends on Reynolds

number, wall curvature, sweep, roughness, and initial conditions. If Fig. 1 is entered with weak disturbances and path *A* is followed, the initial growth of these disturbances is described by *linear* stability theory of *primary* modes (i.e. linearized, unsteady, Navier-Stokes). This growth is weak, occurs over a viscous length scale, and can be modulated by pressure gradients, surface mass transfer, temperature gradients, etc. As the amplitude grows, three-dimensional and nonlinear interactions occur in the form of *secondary* instabilities. Disturbance growth is very rapid in this case (now over a convective length scale) and breakdown to turbulence occurs.

Since the linear stability behavior can be calculated, it is often assumed that transition follows path *A* and transition prediction schemes are usually based on linear theory. This is justified on the assumption that external flows typically have weak freestream disturbances and the region of linear growth is large compared to that of the nonlinear region. However, since the initial conditions (receptivity) are not generally known, only correlations are possible and, most importantly, these correlations must be between two systems with similar environmental conditions. Recent critical reviews of these methods are found in Arnal (1992, 1993) and Reed et al (1996). In general, correlations using linear methods work well in 2-D basic states but do poorly in 3-D basic states.

At times, the freestream disturbances are so strong that the growth of linear disturbances is *bypassed* (Morkovin, 1969, 1991, 1993) and turbulent spots or secondary instabilities occur and the flow quickly becomes turbulent. This corresponds to path *E* in Fig. 1 and while the phenomenon is not well understood it has been documented in cases of roughness and high freestream turbulence (Reshotko, 1984, 1986, 1994). In this case, transition prediction schemes based on linear theory fail completely.

It is generally accepted that bypass refers to a transition process whose initial growth is not described by the primary modes of the Orr-Sommerfeld (O-S) equation. Historically, one had either path *A* or *E* from which to choose as the road to turbulence. Recently however, considerable work has taken place in the area of *transient growth* that expands our understanding of how transition to turbulence can occur.

Transient growth occurs when two, non-orthogonal, stable modes interact, experience a region of algebraic growth, and then decay exponentially. Important modes appear to be streamwise vorticity and wall-normal vorticity which can account for the presence of 3-D modulations of 2-D waves which are necessary for secondary instabilities. This mechanism was first elucidated by Landahl (1980) and then Hultgren and Gustavsson (1981). This idea was exploited by Henningson et al (1993) and others. A recent review of these efforts is given by Andersson et al (1998).

Theoretical and computational studies have shown that large amplitudes can be achieved through transient growth when the boundary layer is provided with the appropriate initial conditions. Thus the spectrum of initial conditions depends on receptivity. Returning to Fig. 1, one can now say that, depending on amplitude, transient growth can lead to spanwise modulations of 2-D waves (path *B*), direct distortion of the basic state which leads to secondary instabilities (path *C*), or direct bypass (path *D*). Note that Fig. 1 narrows the definition of bypass to those mechanisms that resist successful modeling by linear or secondary instability theory.

1.2 Leading-Edge Receptivity

In spite of considerable progress, the theory remains rather incomplete with regard to predicting transition. Amplitude and spectral characteristics of the disturbances inside the laminar viscous layer strongly influence which type of transition occurs. Thus it is necessary to understand how freestream disturbances are entrained into the boundary layer and create the initial amplitudes of unstable waves, i.e., to answer the question of *receptivity*. For the discussion here, the wave instability is assumed to be of the Tollmien-Schlichting (T-S) type and the ultimate goal is to determine how the wave amplitude within the boundary layer can be found from a freestream measurement. Even though the restriction to T-S waves may make this goal seem too modest, one soon finds sufficient challenges for theoretical, computational, and experimental modeling. Thus, transient growth, 3-D boundary layers, 3-D roughness, and bypasses are not discussed here. The role of compressibility is reviewed in Reshotko (1997).

Receptivity has many different paths through which to introduce a disturbance into the boundary layer. They include the interaction of freestream

turbulence and acoustic disturbances (sound) with model vibrations, leading-edge curvature, discontinuities in surface curvature, or surface inhomogeneities. Moreover, the picture for 2-D flows is expected to be different than that of 3-D flows. Any one or a combination of these effects may lead to unstable waves in the boundary layer. The incoming freestream disturbance (sound or turbulence) at wavenumber α_{fs} interacts with a body in such a way (roughness, curvature, etc) so as to broaden its spectrum to include the response wavenumber α_{TS} . If the initial amplitudes of the disturbances are small, they will tend to excite the linear normal modes of the boundary layer. The normal modes in the case of a typical experiment dealing with a Blasius boundary layer are of the T-S type (Mack, 1984). If the initial amplitudes are large, the boundary layer may respond directly to nonlinear 3-D effects that can lead prematurely to transition.

Mathematically, the receptivity problem differs from stability (Reshotko, 1976, 1984, 1994). Stability analysis describes the normal modes of disturbances within the boundary layer. These normal modes are determined from the solution of the linearized Navier-Stokes equations with appropriate boundary conditions (i.e. the O-S equation). The history of the development of this area is given by Mack (1984). Receptivity differs in the fact that either the equations or the boundary conditions are no longer homogeneous since the boundary layer is being forced by an external disturbance. Therefore, the problem no longer has the form of an eigenvalue problem but rather an initial-value problem. The governing system of equations for the receptivity problem is therefore typically the full Navier-Stokes system with appropriate boundary and initial conditions. Thus, the objective of any transition program should address initial conditions for T-S wave generation.

1.3 Rotational and Irrotational Disturbances

Through the work of Kendall (1990, 1991, 1998), it is believed that the *vortical* parts of the freestream disturbances are the contributors to the 3-D aspects of the breakdown process while the work of Kosorygin et al. (1995) showed that the *irrotational* parts of the freestream disturbances contributed to the initial amplitudes of the 2-D Tollmien-Schlichting (T-S) waves. Under some conditions, high-amplitude disturbances do not follow the usual instability route and lead directly to

transition (Morkovin 1993; Reshotko 1994). Thus, sound and turbulence present a different set of problems in the understanding, prediction, and control of transition to turbulence and, as such, require unusual experimental and computational techniques.

Since receptivity deals with the generation rather than the evolution of instability waves in a boundary layer, neither departures from the linear-mode scenario, called *bypass phenomena* (Morkovin 1993; Reshotko 1994), nor details of the transition process itself (Morkovin 1991; Saric 1996) are discussed here. To generate instability waves, energy from the long-wavelength external disturbances must be transferred to the shorter wavelength T-S waves through some kind of *local* (Goldstein et al. 1983a, 1983b, 1989; Kerschen et al. 1990; Crouch 1992a) or *global* (Crouch 1992b) flow adjustment. Fortunately, a number of unique reviews of earlier receptivity research were given recently by Choudhari and Streett (1994), Crouch (1994), Reshotko (1994), Saric et al. (1994), and Wlezien (1994). The reader is referred to these reviews and their references.

Since these reviews, papers have appeared by Breuer et al. (1996), Kobayashi et al. (1995, 1996), and Kato et al. (1997). They deal with different aspects of 3-D wave motion and nonlinearities and are not discussed.

Here we consider disturbances consisting of only plane acoustic waves. We ignore freestream turbulence and artificial disturbances within the boundary layer. Moreover, the main objective of this experiment is to isolate the influence of the leading edge on the initial amplitudes of T-S waves and to determine the limit of linear receptivity for 2-D roughness. The goal is to establish the framework for the active control of such fluid motions and to provide the initial conditions for computational and analytical modeling.

The section on DNS reports on recent advances made in understanding the leading-edge problem. There have been very few experiments and these are reviewed in the last section. This review of receptivity covers freestream turbulence and vortical motions in addition to its primary goal of addressing acoustic receptivity. The report concentrates on low-disturbance environments and 2-D disturbances.

2 THEORY AND COMPUTATIONS

The theory of leading-edge receptivity, in which the work of Goldstein (1983, 1985) has played a seminal role, has led to all of the progress that was later achieved by DNS and experiments. Although Saric et al (1994) review the early work, the references of Goldstein and co-workers, Kerschen and co-workers, Crouch, and Choudhari are given in the references. Saric et al (2000) is an updated and expanded version of Saric et al (1994) and it contains a tutorial on receptivity theory.

Direct numerical simulations (DNS) are playing an increasingly important role in the investigation of transition; the literature is growing, especially recently. This trend will continue as considerable progress is made in the development of new, extremely powerful computers and numerical algorithms. In such simulations, the full Navier-Stokes equations are solved directly by employing numerical methods, such as finite-difference, finite-element, or spectral methods. Kleiser and Zang (1991) and Reed (1993) serve as complementary companions to review temporal and spatial simulation techniques, respectively.

The coupling between the long-wavelength acoustic disturbance and a T-S wave, having wavelengths two orders of magnitude smaller, occurs when the boundary layer is required to adjust locally (Goldstein 1983; Goldstein et al 1983; Goldstein 1985, Goldstein and Hultgren 1989; Heinrich et al 1988; Kerschen 1990; Crouch 1991, 1992a) or globally (Crouch 1992b). This can occur at four positions on a flat-plate model: the leading edge, the discontinuity in the surface curvature occurring at the flat-plate and leading-edge junction, the presence of very strong, localized, pressure gradients, and any surface inhomogeneities.

Experimentally, the most popular receptivity model has been the flat plate with an elliptic leading edge. Thus it is reasonable that computational models consider the same geometry. However, the curvature at the juncture between the ellipse and the flat plate is discontinuous and provides a source of receptivity (Goldstein 1985; Goldstein and Hultgren 1987). Lin et al (1992) introduced a new leading-edge geometry based on a super-ellipse. The shape of this modified super-ellipse (MSE) is given by

$$\left[\frac{(a-x)}{a}\right]^{m(x)} + \left[\frac{y}{b}\right]^n = 1, \quad 0 < x < a \quad (1a)$$

$$m(x) = 2 + \left[\frac{x}{a}\right]^2 \text{ and } n = 2 \quad (1b)$$

where $a = b(AR)$, b is the half-thickness of the plate, and AR is the aspect ratio of the "elliptic" nose. For a usual super-ellipse, both m and n are constants. These super-ellipses will have the advantage of continuous curvature (zero) at the juncture with the flat plate as long as $m > 2$ at $x/b = AR$. The MSE, with $m(x)$ given above, has the advantage of having a nose radius and geometry (hence a pressure distribution) close to that of an ordinary ellipse with $m = 2$ and $n = 2$.

2.1 Receptivity to freestream sound

For low-speed flows, the freestream-sound wavelength is typically one or two orders of magnitude larger than instability wavelengths in the boundary layer. Receptivity is defined to be the rms T-S amplitude at Branch I normalized with the rms freestream-sound amplitude.

$$K_s = \left(\left|u'\right|_{TS}\right)_I / \left(\left|u'\right|_{ac}\right)_{fs} \quad (2)$$

Lin et al (1991, 1992) simulated the receptivity of the laminar boundary layer on a flat plate by solving the full Navier-Stokes equations in general curvilinear coordinates by a second-order finite-difference method with vorticity and stream function as dependent variables. Geometries tested included elliptic, polynomial-smoothed elliptic, and MSE leading edges of different aspect ratios (with smaller aspect ratio corresponding to a blunter nose). Various sound-like oscillations of the freestream streamwise velocity were applied along the boundary of the computational domain and allowed to impinge on the body. Parameters that were varied included disturbance amplitude and frequency, as well as leading-edge radius and geometry. They found the following:

(a) T-S waves appearing in the boundary layer could be linked to sound present in the freestream.

(b) Receptivity occurred in the leading-edge region where rapid streamwise adjustments of the basic flow occurred. Variations in curvature, adjustment of the growing boundary layer, discontinuities in surface geometry, and local pressure gradients there introduce length scales to diffract long freestream disturbances in much the same way as the theory predicted.

(c) The magnitude of receptivity and the disturbance response depended very strongly on geometry. For example:

(i) For plane freestream sound waves, T-S -wave amplitude at Branch I decreased as the elliptic nose was sharpened. However, this is due to the relaxation of the adverse pressure gradient. The receptivity coefficient based on T-S amplitude near the leading edge behaves in an opposite manner.

(ii) When the discontinuity in curvature at the ellipse/flat-plate juncture was smoothed by a polynomial, receptivity was cut in half.

(iii) The disturbance originated from the location of the maximum in adverse pressure gradient.

(d) The receptivity to plane freestream sound appeared to be linear with freestream-disturbance amplitude up to levels of about 5% U_∞ . Thus a linear Navier-Stokes solution could be used up to these levels.

Receptivity coefficients were obtained for a range of frequencies. For example, the values obtained for both a 6:1 and a 20:1 MSE are contained in the table below; the 20:1 geometry is included for comparison with the experiments of Saric and White (1998). The receptivity coefficient, K_s , is defined in Eq. 2 and F is the reduced frequency defined in the nomenclature. The receptivity coefficients have been extrapolated downstream from the numerical results by using linear stability theory. The amplitude of the instability wave was taken at its maximum absolute value within the boundary layer after decomposing using the method presented above. The results of the numerical simulations show no significant variation with frequency. The agreement between the computations and the experiment is excellent, and we conclude that each validates the other.

	K_s	K_s	K_s
F	6:1 MSE	20:1 MSE	20:1 MSE
	DNS	DNS	Experiment
80	0.0030		
82	0.0030	0.048	0.05
84	0.0031	0.048	0.05
86	0.0032	0.048	0.05
88	0.0033		
90	0.0034		

Table 1: Branch I receptivity coefficients for multiple frequencies as predicted by DNS and compared with the experiments of Saric and White (1998).

The results of Haddad and Corke (1998) show that at the leading edge the receptivity coefficient has a value of approximately 0.47 for a Strouhal number based on the nose radius of 0.01 (which is the value in the present numerical simulations). In the theoretical results of Hammerton and Kerschen (1996), the leading-edge receptivity coefficient is found to be nearly unity. The value of the receptivity coefficient at an x -location of 1/2 the wavelength of the associated instability wave (which represents a distance based on the hydrodynamic length scale U/ω of approximately unity) in the present simulations compares well with the theoretical results, predicting a leading-edge value of approximately 0.75. Here U is the speed of the uniform freestream flow and ω is the frequency of the plane acoustic wave. In trying to do these comparisons, certain difficulties arise. Uncertainty exists in the DNS (and experiments) in the choice of streamwise location in the leading-edge region at which the amplitude should be sampled for comparison with the asymptotic theory. Moreover it is often difficult to make direct leading-edge measurements in an experiment because of the scales involved and to separate the Stokes wave from the instability in the DNS in the leading-edge area because both exhibit variation on similar streamwise length scales. Consequently, in the present DNS, we extrapolated linear stability theory forward to $x=4.8$ for the qualitative comparison. These problems are removed when the receptivity coefficient is based on Branch I results, as is seen in the previous paragraph

describing the straightforward and quantitative comparison between DNS and the experiments. Branch I is unambiguous and we recommend that the standard definition of receptivity coefficient be based upon it, especially to aid the community in the evaluation of different theories and numerical and experimental methods in the prediction of receptivity. One has only to keep in mind that pressure recovery region ahead of Branch I influences the T-S amplitude by an amount that can be calculated.

2.2 Non-Symmetric Calculations

Acoustic waves impinging upon the geometry at angles of incidence α_{ac} were investigated. The numerical farfield-boundary condition in the disturbance calculation is modified to include a normal component of the velocity oscillation. This effectively changes the angle of incidence of the impinging acoustic wave. The basic-state solution remains at zero angle of attack. Because the flowfield is no longer symmetric, the full domain must be computed. An oblique acoustic wave causes small-amplitude motion of the stagnation point and thus introduces a small vertical component of velocity at the leading edge. The farfield-boundary location and buffer-zone parameters are systematically varied to show invariance of the numerical solution.

Values of the leading-edge receptivity coefficient for different angles of incidence are determined and plotted in Fig. 2. The decomposition technique is not valid in this region and the amplitudes are found by extrapolating using linear stability theory. The non-dimensional wavelength (based on the half-thickness of the MSE) is approximately 10. Plotted in this same figure are the results of Heinrich and Kerschen (1989). As can be seen there is an increase in the receptivity coefficient with increasing angle of incidence but at a much smaller rate than that predicted by this theory for the zero-thickness flat plate. The slope of the increase in receptivity for the DNS is approximately 0.15 whereas the increase as predicted by Heinrich and Kerschen is approximately 0.65. Therefore the DNS predicts a slope of less than 1/4 of the slope predicted by this theory.

A comparison with the finite-nose-radius theoretical results of Hammerton and Kerschen (1996) shows much more encouraging results. The Strouhal number based on nose radius for the present simulations is 0.01 and Hammerton and Kerschen

(1997) point out that the asymptotic results for small Strouhal number do not apply. Since we are dealing with very low Mach numbers, the results for reduced acoustic frequency

$$k = \frac{\omega b}{c} \ll 1$$

are applied. Here b is the airfoil semi-chord and c is the speed of sound. In other words, the acoustic wavelength is long not only compared to the hydrodynamic length scale U/ω , but also compared to the airfoil chord. From equations (4.3) and (4.9) in Hammerton and Kerschen (1996), the leading-edge receptivity coefficient is defined as

$$C_1(St_r, \alpha_{ac}) = \cos \alpha_{ac} C_s(St_r) + a^{1/2} \sin \alpha_{ac} C_a(St_r)$$

Here C_s and C_a are the symmetric and antisymmetric components of the receptivity coefficient, and $a = \omega b/U$ is the aerodynamic reduced frequency. For the present geometry and freestream conditions, $U/\omega = 4.8$ in units of plate half-thickness and $St_r = 0.01$ based on nose radius. From figures 4 and 5 of Hammerton and Kerschen (1996), the following values are predicted:

$$\begin{aligned} |C_s| &= 1 & \arg C_s &= 0.67\pi \\ \left| \frac{C_a}{C_s} \right| &= 4.9 & \arg \frac{C_a}{C_s} &= 0.2\pi \end{aligned}$$

It is difficult for us to determine a precise value for “ a ” since our geometry is semi-infinite in the downstream direction. Per Hammerton and Kerschen (1996), the following condition must be satisfied in order that their local expansion of the thickness distribution for an airfoil with a rounded leading edge of radius r_n be valid:

$$\frac{b}{L} = O\left(\frac{L}{r_n}\right)$$

Satisfying the strict equality of equation (6) puts our “trailing edge” “far downstream” at $x=40$ in units of half-thickness (away from the influence of the leading edge) and suggests the calculation be done for a value of $a=4.1$. This value gives the following comparison:

α_{ac} (degrees)	C_l DNS	C_l Theory
0	0.75	1.0
5	1.3	1.8
10	2.1	2.6
15	3.2	3.4

Table 2: Leading-edge receptivity coefficients for various incidence angles as predicted by DNS and compared with the finite-nose-radius theory of Hammerton and Kerschen (1996).

The agreement is excellent and (comparing with the poor agreement in Fig. 2) clearly demonstrates the importance of including the effects of the finite nose radius in any receptivity study. [A comparison with Haddad and Corke (1998) is not possible because both their wave and basic state were at incidence.]

3 EXPERIMENTS

A complete review of the early experimental work is reported by Nishioka and Morkovin (1986) in an overview of experiments in boundary-layer receptivity to unsteady pressure gradients. They offer a critical appraisal of acoustically-driven-transition literature and they conclude that all previous experiments were flawed to some extent. More recent reviews of the receptivity research are given by Reshotko (1994), Saric et al. (1994), Wlezien (1994), Choudhari and Streett (1994) and Crouch (1994).

A goal of any receptivity experiment is to follow the four criteria established by Nishioka and Morkovin (1986) where they discuss some of the basic difficulties that have occurred in receptivity experiments using acoustic freestream disturbances. They specifically mention that previous experiments have been inconclusive because of (1) poor quantitative characterization of the forcing field along the outer edge of the boundary layer, (2) inadequate local information on the fluctuations in the boundary layer in the region where the stimulated unstable response starts growing, (3) lack of documentation of potentially singular diffraction fields around the leading edge and/or the singular effects of vibrations of the leading edge, and (4) excessive forcing disturbance levels. Care with (1) and (2) allows different receptivity mechanisms to be

sorted out and attention to (3) and (4) isolates other receptivity paths and nonlinearities. These then are the detailed responses to the caveats of Saric (1990) i.e. get the linear problem correct and provide initial conditions for the theory and computations.

3.1 Measurement techniques

Prior to Kendall (1990), Wlezien (1989), and Wlezien et al (1990), acoustic receptivity measurements suffered from contamination of the T-S signal by background disturbances. If an external sound source is used as a source of disturbance energy, say in a receptivity experiment, then the boundary-layer measurement at a particular frequency will contain probe vibrations and a sound-wave component in addition to the T-S wave. It is easy for external sound to force, at the oscillation frequency, the mechanical system holding the hot wire. The external sound field generates a Stokes layer imbedded inside the boundary layer. If these signals are of comparable amplitude to the T-S amplitude, one does not obtain the usual T-S amplitude profile unless some special technique is used to extract the T-S wave. It is for this reason that older publications do not show typical T-S profiles. Techniques for separating the T-S wave from the sound field are reviewed in Saric (1996).

The details of the experiment are given in Saric and White (1998). One of their most important results explained the narrow pass-band response in receptivity coefficients observed by Saric et al (1995). They showed that reflected sound from the diffuser constructively and destructively interacted with the on-coming sound. They used a pulsed-sound technique

3.2 Pulsed-sound technique

In the current flat-plate experiment, short-duration, planar acoustic pulses in the freestream interact with a 20:1 super ellipse leading edge. The resulting disturbance waves are measured and are used to calculate leading-edge receptivity coefficients. These coefficients, defined in Eq. 2, relate the magnitudes of freestream acoustic disturbances to the magnitudes of the resulting Tollmien-Schlichting (T-S) waves at the Branch I neutral stability point. The receptivity coefficients for a particular freestream speed are functions of the reduced frequency, F , defined in the nomenclature.

In the present experiment, a pulsed-sound forcing technique first proposed by Saric et al. (1995) is implemented to generate receptivity coefficients. This technique was developed to address problems associated with continuous acoustic forcing, specifically the superposition of Stokes waves generated by the continuous freestream acoustic fluctuations on the T-S waves generated via the receptivity phenomenon under investigation. The pulsed-sound technique was used previously by Saric and White (1998) for large-amplitude disturbances, but has since been refined so that very low amplitude disturbances can be effectively measured. The improved sensitivity has been crucial for examining the case of the 20:1 modified super ellipse leading edge. Developing the technique has revealed a number of areas in which the pulsed-sound method is crucial for accurately performing an acoustic receptivity experiment. In many cases, no other existing technique is feasible.

The pulsed-sound receptivity experiments consist of generating very short acoustic input signals, typically two- to four-cycle sine waves, and conditionally sampling the resulting freestream and boundary-layer hot wire signals. The freestream wire measures the primary input pulse and then, depending on the frequencies of input sound, possibly a reflection of the acoustic wave. The boundary-layer hot wire will measure first a Stokes wave coincident with the passage of the acoustic wave and reflection through the test section, then some time later a T-S wave. The delay between the Stokes and T-S waves is generated by the phase speed difference between the acoustic and boundary-layer disturbance signals. The Stokes wave travels at sonic velocity; the T-S wave travels at a fraction of the freestream speed, U_∞ . Since the measurement location is greater than a meter downstream of the leading edge (the only receptivity location), several hundred milliseconds separate the Stokes and T-S signals measured by the boundary-layer wire. Sampling only the second signal in the boundary layer yields separated T-S data. A time trace of the different velocity signals are shown in Fig. 3.

It is necessary to limit the signals used for analysis to avoid echo-induced errors. The diffuser downstream of the test section creates a reflection of the input acoustic pulse which is strongest near 74 Hz. In the freestream, the echo is observed as extra acoustic cycles following the primary input pulse. In the boundary layer, the initial Stokes wave exhibits

the same extra-cycle characteristic, but more importantly, the echo enhances the boundary-layer T-S pulse as well. The receptivity of the leading edge to upstream-travelling acoustic disturbances is expected to be much stronger than to downstream-travelling waves. Since the downstream-travelling waves are of interest here and the T-S waves generated by the echo may be of large amplitude relative to the primary T-S packet, some care must be exercised in removing the echo-induced parts of the signals.

The removal of the echo-induced signal is accomplished by establishing a data-acquisition window triggered by the input sound. To set up the acquisition window, sound pulses are introduced at the most-amplified T-S frequencies. The duration of these test pulses is limited so the primary and echo pulses are clearly separated in both the boundary layer and freestream signal traces. The acquisition window start and end times relative to the input sound trigger are determined manually using an averaging, digital oscilloscope. For sound input at other, less amplified frequencies, the input pulse duration is maintained by changing the number of input cycles so that the window length remains correct even though these off-peak T-S signals are not visible on the oscilloscope. For example, for 15 m/s, the acquisition window is determined using 5-cycle, 110 Hz input sound. Lower frequency excitation is accomplished using either 4-cycle, 88 Hz or 3-cycle, 66 Hz input pulses.

The amplitude measure of the freestream acoustic input and the T-S wave response employed here is the magnitude of the complex Fourier coefficient for each frequency present in the wave packets. Earlier work involving continuous forcing (Saric et al. 1995) used root mean square (rms) disturbance measurements. The Fourier approach yields several benefits. First, for the transient (i.e., noncontinuous forcing) experiment, the rms amplitude of a wave packet is a poorly defined quantity. The acoustic and T-S wave packets both have amplitude envelopes that vary throughout the pulse. Moreover, the frequency-domain approach is in fact the only means to correctly describe the receptivity and linear amplification process of multiple-frequency signals. This is because as wave packets travel downstream, high-frequency components of the spectra, which are present initially due to the finite extent of the pulse, decay. Meanwhile, the low-frequency components in the amplified T-S band grow. The net result in the time domain is a packet that not only has a larger

maximum disturbance amplitude but is also longer. The rms amplitude measure fails to capture this behavior since averaging does not consider the extent of the pulse.

A feature of short sound bursts is that since they are limited in the time domain, they are extended in the frequency domain. Thus, a single sound pulse (a single frequency sine wave within an amplitude envelope) covers a wide frequency range. In many cases the pulse spectrum covers the entire T-S wavelength band. Therefore, using a pulsed-sound approach eliminates the distinction between single frequency and broadband input. Unfortunately, this relationship between short signals and wide frequency bands is responsible for the chief drawback of the pulsed-sound method. Because the data acquisition period is short, results with poor frequency resolution are produced. In typical measurements, the pulse sampling period is 0.256 sec, which gives a fundamental frequency resolution of 3.9 Hz.

A large number of ensemble averages (200--800) are required to obtain the best possible results. The averaging is not of rms values (Saric et al., 1995) or the Fourier coefficient magnitudes (Saric and White 1998), but of the real and imaginary parts of the Fourier coefficient of each frequency separately. Data acquisition is triggered using the signal generator input, so the part of the Fourier coefficients due to the input sound should be of very consistent phase, pulse to pulse. The components of the measured signals that are not due to the forced input are not phase correlated, and are therefore removed by complex averaging. To verify that the part of the signal removed by averaging is truly random, statistics concerning the noise are monitored during the experiment. For the averaging to be valid, the random noise signal, which can be represented for each pulse and frequency as $re^{i\theta}$, must have the phase, θ , uniformly distributed on $(0,2\pi)$ and there must be no correlation between r and θ . Both of these requirements are satisfied for the frequencies of interest in the experiment. The averaged real and imaginary parts form the magnitude of the correlated T-S and acoustic signals. Exploiting the fixed phase of the response relative to the input allows disturbances several orders of magnitude below the random background signal to be measured. Example freestream and boundary-layer spectra generated using the complex averaging technique are shown in Fig. 4.

The T-S waves are measured as far downstream as possible, typically just before the Branch II neutral point, to (1) obtain the strongest possible disturbance signal and (2) generate the greatest separation possible between the Stokes and T-S wave packets. In generating the receptivity coefficients, linear theory is used to relate the T-S amplitudes measured downstream to the amplitudes at the Branch I neutral point. Furthermore, the receptivity coefficients are calculated by assuming that the receptivity process at the leading edge is linear as well, that is, the presence of a particular frequency component in the boundary-layer signal is proportional to the amplitude of that component in the freestream and depends on no other frequency. With the complex averaging technique, linearity can be observed over many orders of magnitude. The linear response of the T-S wave amplitude at 82.0 Hz to the freestream amplitude at the same frequency is shown in Fig. 5

3.3 Leading-edge receptivity results

The pulsed-sound technique has been used to measure T-S mode shapes such as that shown in Fig.6. The observed mode shapes match linear theory predictions and demonstrate convincingly that the pulsed-sound/Fourier technique is a valid means of measuring relative disturbance amplitude. Presently, the leading-edge receptivity coefficients for freestream speeds ranging from 8~m/s (the highest velocity flow which can be compared with DNS results) to 15~m/s have been generated. The results at 8 m/s are compared with DNS in Table 1 in section 2

Figure 4 shows the magnitude-averaged (dashed) and complex-averaged (solid) spectra for 12 m/s freestream speed and 5-cycle, 85~Hz sound pulses. Both averaging methods use 800 ensembles. The higher amplitude curves represent the response to 25% of the maximum possible speaker output. The lower amplitude curves represent 2% speaker output.

Figure 5 shows the linear response of the 82.0 Hz ($F^2=60$) T-S wave to acoustics forcing. Freestream speed is 12 m/s. The amplitude of the $2f$ harmonic at 164.0 Hz is proportional to the square of the amplitude of the fundamental input frequency. The power-law fit for the harmonic was not extended to the two lowest points because these could not be distinguished from the background noise level using 400 ensemble averages.

Figure 6 is the T-S mode shape profile for $U_\infty = 12.5$ m/s and $F=58$ showing excellent agreement between linear theory and experimental results.

CONCLUSIONS

We clearly demonstrate that progress has been made in the understanding of receptivity mechanisms. Theory and experiment agree on 2-D roughness and on leading-edge receptivity coefficient. DNS establishes a viable framework for detailed studies of leading-edge receptivity. Challenges still exist in the areas of freestream turbulence, bypasses, 3-D flows, and compressibility. We expect progress to occur when theoretical, computational, and experimental methods are combined to address these important problems.

ACKNOWLEDGEMENTS

The authors would like to acknowledge the contributions of Dr. Keith Chapman, Dr. David Fuciarelli, Mr. Ian Lyttle, Dr. Ronald Radeztsky and Dr. Mark Reibert during the nascent stage of this work. Professor Edward Kerschen has always been ready to offer advice and suggestions on all aspects of this work for which we are grateful. The continuous help and assistance of Mr. Dan Clevenger and Ms Colleen Leatherman is greatly appreciated.

This work was sponsored (in part) by the Air Force Office of Scientific Research, USAF, under *Grant Number F49620-96-1-0369*. The support of E.B.W. through the ASU University Graduate Scholar program and the Allied Signal Fellowship program is gratefully acknowledged. The acoustic speakers were donated by McCauley Sound Inc., Puyallup, Washington.

REFERENCES

- Alfredsson, P.H., Matsubara, M. 1996 Streaky structures in transition. In *Proc. Transitional Boundary Layers in Aeronautics*. (R.A.W.M. Henkes, J.L. van Ingen, editors), pp. 373-386, Royal Netherlands Academy of Arts and Sciences. Elsevier Science Publishers.
- Arnal, D. 1992 Boundary-layer transition: Prediction, application to drag reduction. *Special Course on Skin Friction Drag Reduction, AGARD Report 786*, March 1992.
- Arnal, D. 1993 Predictions based on linear theory. *Progress in Transition Modelling, AGARD Report 793*, March 1993.
- Arnal, D., Juillen, J.C. 1978 Contribution experimentale a l'etude de la receptivite d'un couche limite laminaire, a la turbulence de l'ecoulement general. *ONERA Rt. Tech. no. 1/5018 AYD*.
- Ashpis, D.E., Reshotko, E. 1990 The vibrating ribbon problem revisited. *J. Fluid Mech.*, **213**, 531.
- Bayley, B.J., Orszag, S.A., Herbert, T. 1988 Instability mechanisms in shear-flow transition. *Ann. Rev. Fluid Mech.* **20**, 359.
- Bodonyi, R.J. 1990 Nonlinear triple-deck studies in boundary-layer receptivity. *Appl. Mech. Rev.*, **43**, no.5, part 2, S158.
- Bodonyi, R.J., Welch, W.J.C., Duck, P.W., Tadjfar, M. 1989 A numerical study of the interaction between unsteady freestream disturbances and localized variations in surface geometry. *J. Fluid Mech.*, **209**, 285.
- Breuer, K.S., Grimaldi, M.E., Gunnarsson, J., Ullmar, M. 1996 Linear and nonlinear evolution of boundary layer instabilities generated by acoustic receptivity mechanisms. *AIAA Paper 96-0183*.
- Buter, T.A., Reed, H.L. 1994. Boundary-layer receptivity to freestream vorticity. *Phys. Fluids* **6** (10) 3368-79.
- Casalis, G., Cantaloube, B. 1994. Receptivity by direct numerical simulation. *Proceedings of ERCOFTAC*, March.
- Choudhari, M. 1992. Boundary-layer receptivity due to distributed surface imperfections of a deterministic or random nature. *Theor. Comp. Fluid Dyn.* **4**, 1.
- Choudhari, M., Kerschen, E.J. 1990. Instability wave patterns generated by interaction of sound waves with three-dimensional wall suction or roughness. *AIAA Paper 90-0119*.
- Choudhari, M., Streett, C. 1992 A finite Reynolds number approach for the prediction of boundary-layer receptivity in localized regions. *Phys. Fluids A*, **4**, 2495.
- Choudhari, M., Streett, C. 1994 Theoretical predictions of boundary layer receptivity. *AIAA Paper 94-2223*.

- Corke, T.C. 1990. Effect of controlled resonant interactions and mode detuning on turbulent transition in boundary layers. *Laminar-Turbulent Transition, Vol. III*, Eds. D. Arnal, R. Michel, Springer-Verlag.
- Cowley, S. 1993. Asymptotic methods and weakly nonlinear theory. *Progress in Transition Modelling, AGARD Report 793*, March 1993.
- Crouch, J.D. 1991. Initiation of boundary-layer disturbances by nonlinear mode interactions. *Boundary Layer Stability and Transition to Turbulence, FED-Vol. 114*, Eds: D.C. Reda, H.L. Reed, R. Kobayashi, ASME.
- Crouch, J.D. 1992a Localized receptivity of boundary layers. *Phys. Fluids A* **4**, 1408.
- Crouch, J.D. 1992b Non-localized receptivity of boundary layers. *J. Fluid Mech.*, **244**, 567.
- Crouch, J.D. 1993 Receptivity of three-dimensional boundary layers. *AIAA Paper 93-0074*.
- Crouch, J.D. 1994 Receptivity of boundary layers. *AIAA Paper 94-2224*.
- Fasel, H.F. 1990 Numerical simulation of instability and transition in boundary layer flows. *Laminar-Turbulent Transition, Vol III*, Eds. D. Arnal, R. Michel, Springer-Verlag, Berlin.
- Fuciarelli, D.A., Reed, H.L. 1994 Direct Numerical Simulations of Leading-Edge Receptivity to Freestream Sound. *Application of Direct and Large Eddy Simulation to Transition and Turbulence, AGARD CP 551*, 29-1.
- Fuciarelli, D.A., Reed, H.L., Lyttle, I. 1998 DNS of Leading-Edge Receptivity. *AIAA Paper 98-2644*, in press, *AIAA J.*
- Gaster, M. 1965 On the generation of spatially growing waves in a boundary layer. *J. Fluid Mech.*, **213**, 531.
- Gaster, M. 1974 On the effects of boundary-layer growth on flow stability. *J. Fluid Mech.*, **66**, 465.
- Gaster, M, Grant, I. 1975 An experimental investigation of the formation and development of a wave packet in a laminar boundary layer. *Proc. R. Soc. Lond.*, **A 347**, 253.
- Gatski, T.B., Grosch, C.E. 1987 Numerical experiments in boundary-layer receptivity, *Proceedings of the Symposium on the Stability of Time-Dependent and Spatially Varying Flows*, Springer-Verlag, 82-96.
- Goldstein, M.E. 1983 The evolution of Tollmien-Schlichting waves near a leading edge. *J. Fluid Mech.*, **127**, 59.
- Goldstein, M.E. 1985. Scattering of acoustic waves into Tollmien-Schlichting waves by small streamwise variations in surface geometry. *J. Fluid Mech.*, **154**, 485.
- Goldstein, M.E., Hultgren, L.S. 1987 A note on the generation of Tollmien-Schlichting waves by sudden surface-curvature change. *J. Fluid Mech.*, **181**, 519.
- Goldstein, M.E., Hultgren, L.S. 1989 Boundary-layer receptivity to long-wave disturbances. *Ann. Rev. Fluid Mech.*, **21**, 137.
- Goldstein, M.E., Leib, S.J., Cowley, S.J. 1987 Generation of Tollmien-Schlichting waves on interactive marginally separated flows. *J. Fluid Mech.*, **181**, 485.
- Goldstein, M.E., Sockol, P.M., Sanz, J. 1983 The evolution of Tollmien-Schlichting waves near a leading edge. Part 2. Numerical determination of amplitudes. *J. Fluid Mech.*, **129**, 443.
- Gulyaev, A.N., Kozlov, V.E., Kuznetsov, V.R., Mineev, B.I., Sekundov, A.N. 1989 Interaction of a laminar boundary layer with external turbulence. *Izv. Akad. Nauk SSR, Mekh. Zhid. Gaza* **5**, 55 (in Russian, English translation in *Fluid Dyn.* **24**:5 700 (1990)).
- Haddad, O., Corke, T.C. 1998 Boundary layer receptivity to freestream sound on parabolic bodies. in press *J. Fluid Mech.*
- Hammerton, P.W., Kerschen, E.J. 1991 The effect of nose bluntness on leading-edge receptivity, *Bull. Amer. Phys. Soc.* **36**, 2618.
- Hammerton, P.W., Kerschen, E.J. 1992 Effect of nose bluntness on leading-edge receptivity. *Stability, Transition and Turbulence*, eds. M.Y. Hussaini, A. Kumar, C.L. Streett Springer-Verlag, New York.
- Hammerton, P.W., Kerschen, E.J. 1996 Boundary-layer receptivity for a parabolic leading edge. *J. Fluid Mech.* **310**, 243-67.
- Hammerton, P.W., Kerschen, E.J. 1997 Boundary-layer receptivity for a parabolic leading edge. Part 2. The

- small Strouhal number limit. *J. Fluid Mech.* 353, 205-220.
- Heinrich, R.A. 1989 Flat-plate leading-edge receptivity to various freestream disturbance structures. *PhD Thesis*, Univ. Arizona.
- Heinrich, R.A., Kerschen, E.J. 1989 Leading-edge boundary-layer receptivity to freestream disturbance structures. *ZAMM*, **69**, T596.
- Heinrich, R.A., Choudhari, M., Kerschen, E.J. 1988 A comparison of boundary-layer receptivity mechanisms. *AIAA Paper 88-3758*.
- Henningson, D.S., Lundbladh, A., Johansson, A.V. 1993 A mechanism for bypass transition from localized disturbances in wall bounded shear flows. *J. Fluid Mech.* **250** pp. 169.
- Herbert, Th. 1991 Boundary-layer transition - analysis and prediction revisited, *AIAA Paper 91-0737*.
- Herbert, T. 1993 Parabolized stability equations. *Progress in Transition Modelling, AGARD Report 793*, March 1993.
- Hultgren, L.S., Gustavsson, L.H. 1981 Algebraic growth of disturbances in a laminar boundary layer. *Phys. Fluids* **24**, pp. 100.
- Kachanov, Yu.S., Kozlov, V.V., Levchenko, V.Ya. 1978 Origin of Tollmien-Schlichting waves in boundary layers under the influence of external disturbances (in Russian). *Mek. Zhid. i Gaza*, **5**, 85. (see *Fluid Dyn.*, 1979, 704.)
- Kato, T., Fukunishi, Y., Kobayashi, R. 1997 Artificial control of the three-dimensionalization process of T-S waves I boundary-layer transition. *JSME Int'l J., Ser. B*, Vol. 40, No. 4, pp 536-41.
- Kendall, J.M. 1982 Study of the effect of freestream turbulence upon disturbances in the pre-transitional laminar boundary layer. *AFWAL-TR-82-3002*.
- Kendall, J.M. 1984 Experiments on the generation of Tollmien-Schlichting waves in a flat plate boundary layer by weak freestream turbulence. *AIAA Paper 84-0011*.
- Kendall, J.M. 1985 Experimental study of disturbances produced in a pre-transitional laminar boundary layer by weak freestream turbulence. *AIAA Paper 85-1695*.
- Kendall, J.M. 1998 Experiments on boundary-layer receptivity to freestream turbulence. *AIAA Paper 98-0530*.
- Kendall, J.M. 1990 Boundary layer receptivity to freestream turbulence. *AIAA Paper 90-1504*.
- Kendall, J.M. 1991 Studies on laminar boundary-layer receptivity to freestream turbulence near a leading edge. *Boundary Layer Stability and Transition to Turbulence, FED-Vol. 114*, 23. Eds: D.C. Reda, H.L. Reed, R. Kobayashi, ASME.
- Kendall, J.M. 1992 Boundary layer receptivity to weak freestream turbulence. *Transition Study Group Notes*, Montana State Univ., July 1994.
- Kerschen, E.J. 1989 Boundary-layer receptivity. *AIAA Paper 89-1109*.
- Kerschen, E.J. 1990 Boundary-layer receptivity theory. *Appl. Mech. Rev.*, **43**, No. 5, part 2, S152.
- Kerschen, E.J. 1991 Linear and nonlinear receptivity to vortical freestream disturbances. *Boundary Layer Stability and Transition to Turbulence, FED-Vol. 114*, Eds: D.C. Reda, H.L. Reed, R. Kobayashi, ASME.
- Kerschen, E.J., Choudhari, M., Heinrich, R.A. 1990 Generation of boundary instability waves by acoustic and vortical freestream disturbances. *Laminar-Turbulent Transition, Vol. III*, Eds. D. Arnal, R. Michel, Springer-Verlag.
- Klebanoff, P.S. 1971 Effect of freestream turbulence on the laminar boundary layer. *Bull. Amer. Phys. Soc.*, **10**, no. 11, 1323.
- Kleiser, L., Zang, T.A. 1991 Numerical simulation of transition in wall-bounded shear flows. *Ann. Rev. Fluid Mech.*, **23**, 495.
- Kobayashi, R., Fukunishi, Y., Kato, T. 1996 Laminar flow control of boundary layers utilizing acoustic receptivity. *Sixth Asian Congress of Fluid Mechanics*, Singapore, Vol.1, pp 629-32.
- Kobayashi, R., Fukunishi, Y., Nishikawa, T., Kato, T. 1995 The receptivity of flat-plate boundary layers with two-dimensional roughness elements to freestream sound and its control. *Laminar-Turbulent Transition, Vol. IV*, Ed. R. Kobayashi, Springer.

- Kosorygin, V.S., Polyakov, N.F. 1990 Autodestruction of unstable waves in a laminar boundary layer (in Russian). *Preprint 11-90, ITPM, Akad. Nauk USSR, Sib. Otd., Novosibirsk.*
- Kosorygin, V.S., Levchenko, V.Ya., Polyakov, N.F. 1988 The laminar boundary layer in the presence of moderately turbulent freestream. (in Russian). *Preprint 16-88, ITPM, Akad. Nauk USSR, Sib. Otd., Novosibirsk.*
- Kosorygin, V.S., Radeztsky, R.H., Jr., Saric, W.S. 1995 Laminar boundary layer sound receptivity and control. *Laminar-Turbulent Transition, Vol. IV*, Ed. R. Kobayashi, Springer.
- Landahl, M.T. 1980 A note on an algebraic instability of inviscid parallel shear flows. *J. Fluid Mech.* **22**, pp. 679.
- Lin, N., Reed, H.L., Saric, W. S. 1990 Leading-edge receptivity to sound: Navier-Stokes computations. *Appl. Mech. Rev.*, **43**, no.5, part 2, S175.
- Lin, N., Reed, H.L., Saric, W. S. 1991 Leading-edge receptivity: Navier-Stokes computations. *Proc. R.A.S. Boundary Layer Transition and Control*, Cambridge, UK, ISBN 0 903409 86 0.
- Lin, N., Reed, H.L., Saric, W.S. 1992 Effect of leading edge geometry on boundary-layer receptivity to freestream sound. *Stability, Transition and Turbulence*, eds. M.Y. Hussaini, A. Kumar, C.L. Streett Springer-Verlag, NY.
- Mack, L.M. 1975 Linear stability theory and the problem of supersonic boundary-layer transition. *AIAA J.* **13**, 278.
- Mack, L.M. 1984 Boundary-layer linear stability theory. *Special Course on Stability and Transition of Laminar Flows, AGARD Report No. 709*, March 1984.
- Morkovin, M.V. 1969 On the many faces of transition. *Viscous Drag Reduction* ed.: C.S. Wells, Plenum.
- Morkovin, M.V. 1978 Instability, Transition to turbulence and predictability. *AGARDograph 236*.
- Morkovin, M.V. 1983 Understanding transition to turbulence in shear layers. *AFOSR-TR-83-0931*.
- Morkovin, M.V. 1991 Panoramic view of changes in vorticity distribution in transition instabilities and turbulence. *Boundary Layer Stability and Transition to Turbulence, FED-Vol. 114*, 1. Eds: D.C. Reda, H.L. Reed, R. Kobayashi, ASME.
- Morkovin, M.V. 1993 Bypass-transition research: Issues and philosophy. *Instabilities and Turbulence in Engineering Flows*, Eds: D.E. Ashpis, T.B. Gatski, R. Hirsh, Kluwer Academic.
- Murdock, J.W. 1980 The generation of Tollmien-Schlichting wave by a sound wave. *Proc. R. Soc. Lond.*, **A 372**, 517.
- Murdock, J.W. 1981 Tollmien-Schlichting waves generated by unsteady flow over parabolic cylinders, *AIAA Paper 81-0199*.
- Nayfeh, A.H., Ashour, O.N. 1994 Acoustic receptivity of a boundary layer to Tollmien-Schlichting waves resulting from a finite-height hump at finite Reynolds numbers. *Phys. Fluids A* **6**, 3705.
- Nishioka, M., Morkovin, M.V. 1986 Boundary-layer receptivity to unsteady pressure gradients: Experiments and overview. *J. Fluid Mech.* **171**, 219.
- Parekh, D.E., Pulvin, P., Wlezien, R.W. 1991 Boundary-layer receptivity to convected gusts and sound. *Boundary Layer Stability and Transition to Turbulence, FED-Vol. 114*, pp 69-75. Eds: D.C. Reda, H.L. Reed, R. Kobayashi, ASME.
- Radeztsky, R.H. Jr., Reibert, M.S., Saric, W.S., Takagi, S. 1993 Effect of micron-sized roughness on transition in swept-wing flows. *AIAA Paper 93-0076*.
- Reed, H.L. 1993 Direct numerical simulation of transition: The spatial approach. *Progress in Transition Modelling, AGARD Report 793*, March 1993.
- Reed, H.L., Saric, W.S. 1989 Stability of three-dimensional boundary layers. *Ann. Rev. Fluid Mech.*, **21**, 235.
- Reed, H.L., Haynes, T.S., Saric, W.S. 1998 CFD validation issues in transition modeling. *AIAA J.*, Vol 36, No. 5, pp 742-51.
- Reed, H.L., Saric, W.S., Arnal, D. 1996 Linear Stability Theory Applied to Boundary Layers. *Ann. Rev. Fluid Mech. Vol. 28*, pp. 389-428.
- Reshotko, E. 1976 Boundary-layer stability and transition. *Ann. Rev. Fluid Mech.* **8**, 311.
- Reshotko, E. 1984 Environment and receptivity. *Special Course on Stability and Transition of Laminar Flows, AGARD Report No. 709*, March 1984.

- Reshotko, E. 1985 Control of boundary-layer transition. *AIAA Paper 85-0562*.
- Reshotko, E. 1986 Stability and transition: What do we know? *Proc. U.S. Nat'l. Congress Appl. Mech.* Austin, TX, ASME, 421.
- Reshotko, E. 1994 Boundary layer instability, transition, and control. *AIAA Paper 94-0001*.
- Reshotko, E., Saric, W.S., Nagib, H. 1997 Flow quality issues for large wind tunnels. *AIAA Paper 97-0225*.
- Rogler, H.L., Reshotko, E. 1975 Disturbances in a boundary layer introduced by a low intensity array of vortices. *SIAM J. Appl. Math.* **28**, 431.
- Saric, W.S. 1990. Low-speed experiments: Requirements for stability measurements. *Instability and Transition, Vol I*, Ed: Y. Hussaini, Springer-Verlag, 1990, 174.
- Saric, W.S. 1992a. Laminar-turbulent transition: Fundamentals. *Special Course on Skin Friction Drag Reduction, AGARD Report 786*, March 1992.
- Saric, W.S. 1992b. The ASU transition research facility. *AIAA Paper 92-3910*.
- Saric, W.S. 1996 Low-Speed Boundary Layer Transition Experiments. *Transition: Experiments, Theory & Computations*. Eds. T.C. Corke, G. Erlebacher, M.Y. Hussaini, ICASE Lecture Notes. Copies are available from the author.
- Saric, W.S., Rasmussen, B.K. 1992. Boundary-layer receptivity: Freestream sound on an elliptical leading edge. *Bull. Am. Phys. Soc.*, **37**, 1720.
- Saric, W.S., Thomas, A.S.W. 1984. Experiments on the subharmonic route to turbulence in boundary layers. *Turbulence and Chaotic Phenomena in Fluids*, Ed. T. Tatsumi, Amsterdam: North-Holland.
- Saric, W.S., Hoos, J.A., Radeztsky, R.H. Jr. 1991. Boundary-layer receptivity of sound with roughness. *Boundary Layer Stability and Transition, FED-Vol. 114*, Eds: D.C. Reda, H.L. Reed, R. Kobayashi, ASME.
- Saric, W.S., Reed, H.L., Kerschen, E.J. 1994 Leading-edge receptivity to sound: Experiments, DNS, theory. *AIAA Paper 94-2222*.
- Saric, W.S., Wei, W., Rasmussen, B.K., Krutckoff, T.K. 1995 Experiments on Leading-Edge Receptivity to Sound. *AIAA Paper 95-2253*.
- Saric, W.S., White, E.B. 1998 Influence of high-amplitude noise on boundary-layer transition to turbulence. *AIAA Paper 98-2645*.
- Saric, W.S., Reed, H.L., Kerschen, E.J. 1994 Boundary-layer receptivity to freestream disturbances. *Ann. Rev. Fluid Mech. Vol. 32*.
- Singer, B.A., Reed, H.L., Ferziger, J.H. 1986 Investigation of the effects of initial disturbances on plane channel transition. *AIAA Paper 86-0433*.
- Singer, B.A., Reed, H.L., Ferziger, J.H. 1989 Effect of streamwise vortices on transition in plane channel flow. *Phys. Fluids A*, **1**, 1960.
- Spencer, S.A., Saric, W.S., Radeztsky, R.H. Jr. 1991 Boundary-layer receptivity: Freestream sound with 3-D roughness. *Bull. Amer. Phys. Soc.*, **36**, 2618.
- Suder, K. O'Brien, J., Reshotko, E. 1988 Experimental study of bypass transition in a boundary layer. NASA-TM-100913.
- Tadjfar, M., Bodonyi, R.J. 1992 Receptivity of a laminar boundary layer to the interaction of a three-dimensional roughness element with time-harmonic freestream disturbances. *J. Fluid Mech.*, **242**, 701.
- Tadjfar, M., Reda, D.C. 1992. Experimental investigation of non-localized receptivity due to acoustic/2-D wavy wall interactions. *Bull. Am. Phys. Soc.* **37**, 1720.
- Tam, C.K.W. 1981. The excitation of Tollmien-Schlichting waves in low subsonic boundary layers to freestream sound waves. *J. Fluid Mech.*, **109**, 483.
- Westin, K.J.A., Henkes, R.A.W.M. 1997. Application of turbulence models to bypass transition. *J. Fluids Eng.* **119**, pp. 859.
- Westin, K.J.A., Boiko, A.V., Klingmann, B.G.B., Kozlov, V.V., Alfredsson, P.H. 1994. Experiments in a boundary layer subject to free-stream turbulence. Part I: Boundary layer structure and receptivity. *J. Fluid Mech.* **281**, pp. 193.
- Wiegel, M., Wlezien, R.W. 1992. Measurement of acoustic receptivity at distributed waviness. *Bull. Am. Phys. Soc.*, **37**, 1720.

Wlezien, R.W. 1989. Measurement of boundary layer receptivity at suction surfaces. *AIAA Paper 89-1006*.

Wlezien, R.W. 1994 Measurement of acoustic receptivity. *AIAA Paper 94-2221*.

Wlezien, R.W., Wiegel, M. 1992. Influence of surface geometry and wavelength detuning on distributed acoustic receptivity. *Bull. Am. Phys. Soc.*, **37**, 1719.

Wlezien, R.W., Parekh, D.E., Island, T.C. 1990. Measurement of acoustic receptivity at leading edges and porous strips. *Appl. Mech. Rev.*, **43**, S167.

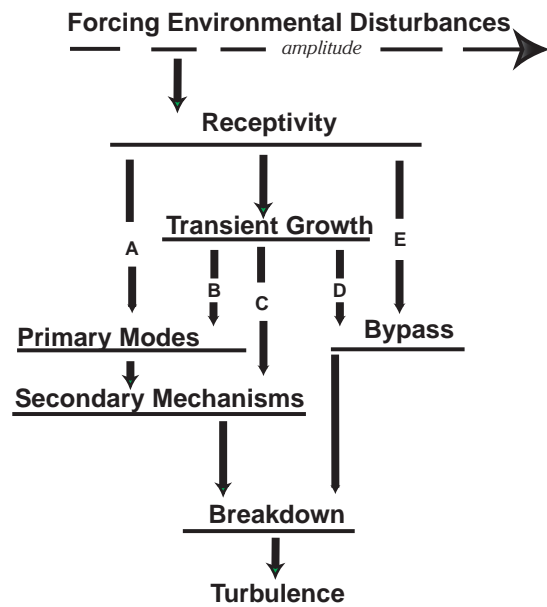


Figure 1. Paths to turbulence

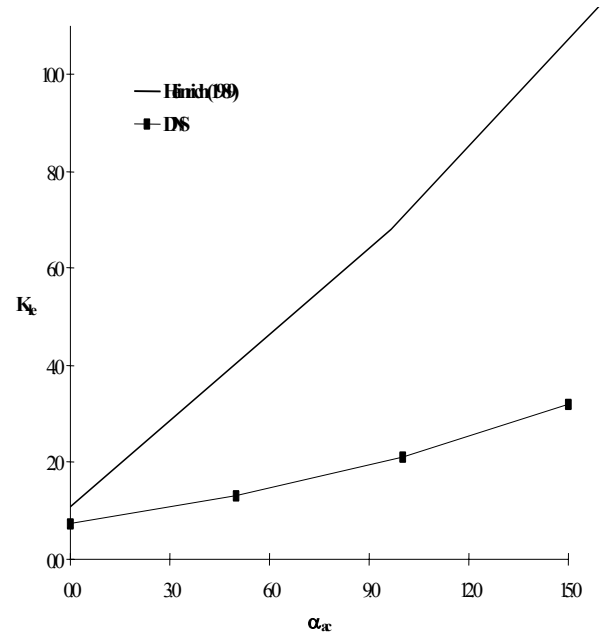


Figure 2. Leading-edge receptivity coefficient as function of acoustic angle of incidence (in degrees). Theoretical results of Heinrich & Kerschen (1989) are for zero-thickness flat-plate at freestream Mach number $M = 0.01$. DNS results are for $Re = 2400$, $F = 86 \times 10^{-6}$, 6:1 MSE.

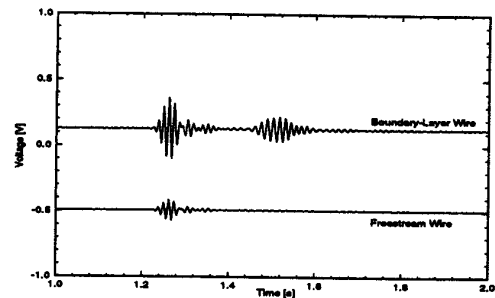


Figure 3. Time traces of freestream wave and boundary-layer wave.

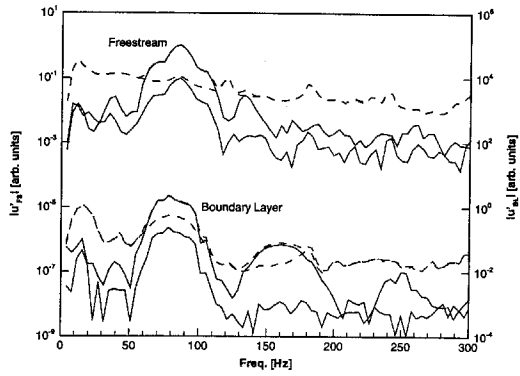


Figure 4. The magnitude-averaged (dashed) and complex-averaged (solid) spectra for 12 m/s freestream speed and 5-cycle, 85-Hz sound pulses.

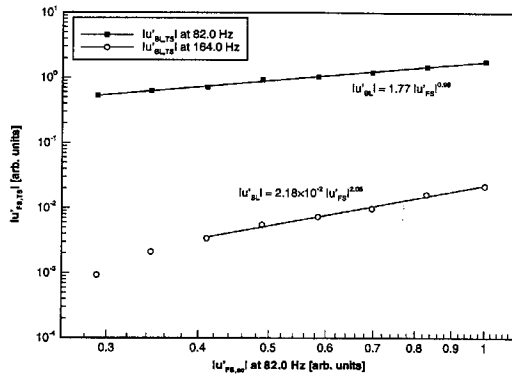


Figure 5. The linear response of the 82.0 Hz ($F=60$) T-S wave to acoustics forcing.

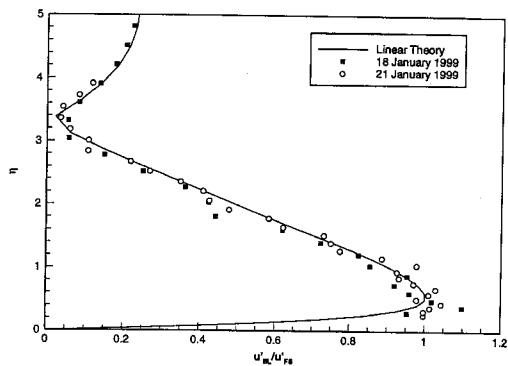


Figure 6. The T-S mode shape profile for $U_{\infty} = 12.5$ m/s and $F=58$